Title: Microstructural changes in white matter associated with freezing of gait in Parkinson's disease

Running title: FOG-related white matter changes

Authors: Vercruysse S, PhD[1,*], Leunissen I, PhD[2,*], Vervoort G, MSc[1], Vandenberghe W, MD[3], Swinnen S P, PhD[2], Nieuwboer A, PhD[1]. ([*]joint first authors)

Affiliations:

[1]Katholieke Universiteit Leuven, Department of Rehabilitation Sciences, Leuven, Belgium

[2]Katholieke Universiteit Leuven, Department of Kinesiology, Leuven, Belgium

[3]University Hospitals Leuven, Department of Neurology, Leuven, Belgium

Please address all correspondence to:

Prof. Alice Nieuwboer

Address: K.U.Leuven, Faculty of Kinesiology and Rehabilitation Sciences, Department of Rehabilitation Sciences, Tervuursevest 101, 3001 Leuven, Belgium

E-mail: allice.nieuwboer@faber.kuleuven.be

Phone: +32-16-32.91.19 ; Fax: +32-16-32.91.15

Word count :

Word count of the manuscript: 2983 words

Number of tables: 3; Number of figures: 2

Supplementary material: yes

Key words:

Parkinson's disease; Diffusion tensor imaging; Freezing of gait; white matter; basal ganglia

Financial Disclosure / Conflict of interest statement:

Support for this study was provided through a grant from the Special Research Fund of KU Leuven, Belgium (contract OT / 11/ 09 and the Malou-Malou funds King Baudouin foundation. I. L. is

supported by a research grant of the Research Foundation – Flanders (F.W.O). Conflict of Interest: All authors report no conflict of interest. W.V. is a Senior Clinical Investigator of the F.W.O.

Abstract (250 words)

Background: In Parkinson's disease (PD), freezing of gait is associated with widespread functional and structural grey matter changes throughout the brain. Previous study of freezing-related white matter changes was restricted to brainstem and cerebellar locomotor tracts.

Objective: To determine the spatial distribution of white matter damage associated with freezing of gait by combining whole brain and striatofrontal seed-based diffusion tensor imaging.

Methods: Diffusion-weighted images were collected in 26 PD patients and 16 age-matched controls. PD groups with (n=11) and without freezing of gait (n=15) matched for age and disease severity. We applied tract-based spatial statistics to compare fractional anisotropy and mean diffusivity of white matter structure across the whole brain between groups. Probabilistic tractography was used to evaluate fractional anisotropy and mean diffusivity of key subcortico-cortical tracts.

Results: Tract-based spatial statistics revealed decreased fractional anisotropy in PD with freezing of gait in bilateral cerebellar and superior longitudinal fascicle clusters. Increased mean diffusivity values were apparent in the right internal capsule, superior frontal cortex, anterior corona radiata, the left anterior thalamic radiation and cerebellum. Tractography showed consistent white matter alterations in striatofrontal tracts through the putamen, caudate, pallidum, subthalamic nucleus and in connections of the cerebellar peduncle with subthalamic nucleus and pedunculopontine nucleus bilaterally.

Conclusions: Freezing of gait is associated with diffuse white matter damage involving major cortico-cortical, corticofugal motor and several striatofrontal tracts in addition to previously described cerebello-pontine connectivity changes. These distributed white matter abnormalities may contribute to the motor and non-motor correlates of freezing of gait.

Introduction

Freezing of gait (FOG) is a disabling gait disorder in Parkinson's disease (PD)[1, 2], which is defined as 'a *brief, episodic absence or marked reduction of forward progression of the feet despite the intention to walk*'[3]. FOG represents an important clinical problem of which the cerebral mechanisms are incompletely understood[3, 4].

In congruence with the variety of motor, cognitive and postural comorbidity of FOG, widespread changes in brain structure and function have been linked with its pathology[5, 6]. Comparing patients with freezing to non-freezing counterparts, functional metabolism studies revealed alterations in orbitofrontal and parietal blood flow[7, 8] and abnormal glucose and dopamine uptake in striatal and parietal regions[9]. Altered functional connectivity in an attention-regulating frontoparietal network, a visual occipito-temporal network and a supplementary motor area-mediated locomotor network was associated with more severe FOG[10, 11]. These functional changes in the brain's resting state may also underlie the disturbed patterns of brain activity and connectivity found in freezers during task preparation and performance. Two studies showed differential activation of the mesencephalic locomotor region and supplementary motor area in patients with FOG compared to those without during imagined walking[12, 13]. Freezers also recruited striatofrontal areas differently than non-freezers during rhythmical movement of the lower and upper limbs[14, 15]. Recent studies pointed to disturbed neuronal activation in basal ganglia and frontoparietal regions during the course of freezing episodes in the limbs and in gait[15-20]. Despite the different methodological paradigms and neuroimaging techniques used, all this work suggests that a dysfunction of higher-order brain centers in conjunction with midbrain and brainstem regions involved in the dynamic and rhythmical control of gait[3] and other movements[21], are implicated in FOG. A similar view stems from structural imaging studies revealing reduced grey matter volume in frontal, precentral sensorimotor, posterior parietal regions[22-24] and brainstem pathology[12] in freezers.

The few structural imaging studies, that examined the freezing-related microstructure of white matter tracts, predominantly focusing on brainstem locomotor regions, yielded altered white matter connectivity in corticopontine and pontine-cerebellar tracts in freezers[25, 26]. Most recently, no differences in preselected subcortical white matter tracts connected to the supplementary motor area were found between small groups of freezers and non-freezers[11]. Therefore, the goal of this study was to capture the extent of FOG-related abnormalities in white matter structure using diffusion tensor imaging (DTI), combining whole brain with tract-based analysis involving the basal ganglia.

Methods

Participants

We studied 26 patients with PD from the Movement Disorders Clinic of the University Hospital Leuven and 15 healthy age-matched controls. Subjects were recruited by a neurologist specialized in movement disorders according to the UK Brain Bank criteria as part of a previous fMRI study[15]. Patients with (N=11) and without FOG (N=15) were matched for age and disease duration. A score ≥ 1 on the New FOG-Questionnaire (NFOG-Q) classified a participant as 'freezer' and a score of 0 as 'non-freezer'[27]. Table 1 provides the clinical details of all participants. Disease severity was assessed by an experienced researcher using the motor section of the Unified Parkinson's Disease Rating Scale (UPDRS III)[28] and Hoehn and Yahr staging[29] while on medication. Patients with a deep brain stimulator or excessive rest tremor were excluded. None of the participants were diagnosed with a neurological disease other than PD or demonstrated a Mini Mental State Examination (MMSE) score ≤ 24. MMSE scores and the cognitive section of the Scales for Outcomes in PD (SCOPA-COG)[30] were lower in PD with FOG than controls but comparable to PD without FOG. Clinical profiles were otherwise similar, except for a higher Levodopa equivalent dose (LED) in freezers compared to non-

freezers. Participants gave informed consent consistent with the sixth version of the Declaration of Helsinki. Ethics approval was received by the local Medical Ethics Committee of the University Hospitals Leuven.

Table 1: Clinical details of participants

		PD with FOG (N=11)	PD without FOG (N=15)	Controls (N=15)	P-value
Gender *(M/F)*	Frequencies[1]	8/3	11/4	11/4	0.98
Age *(years)*	Mean *(SD)*[2]	68.6 *(8.7)*	67.6 *(5.6)*	68.1 *(6.5)*	0.99
MMSE *(0-30)*	Mean *(SD)*[2]	27.2 *(3.1)*	28.3 *(1.4)*	29.6 *(0.6)*	0.01*
SCOPA-COG *(0-43)*	Mean *(SD)*[2]	25.9 *(6.6)*	28.9 *(3.8)*	31.3 *(5.4)*	0.05
Disease duration *(years)*	Mean *(SD)*[2]	9.5 *(3.7)*	7.6 *(5.3)*		0.34
Hoehn and Yahr stage *(0-5)*	Median *(IQR)*[3]	3 *(2.25-3)*	2.5 *(2-2.5)*		0.15
UPDRS III *(0-108)*	Mean *(SD)*[2]	36.6 *(18.3)*	32.5 *(9.1)*		0.47
LED *(mg/day)*	Mean *(SD)*[2]	703.8 *(183.0)*	461.3 *(203.2)*		0.01*
FOG-Q *(0-23)*	Median *(IQR)*[3]	15 *(12.5-19.5)*	0 *(0-0)*		<0.01*

Table 1: Clinical details of participants

* Groups significantly different at p <0.05. SD: Standard Deviation. IQR: Inter-Quartile Range (Q1-Q3). [1]Chi-Square test was used. [2]One-way ANOVA (3 groups) or two-sample t-test was used. [3]Non-parametric Mann-Whitney U test was used. MMSE: Mini Mental State Examination. SCOPA-COG: Scales for Outcomes in Parkinson's Disease- Cognitive part. UPDRS motor score: Unified Parkinson's Disease Rating Scale part III (motor examination); LED: Levodopa Equivalent Dose. FOG-Q: Freezing of Gait Questionnaire.

MRI data acquisition

A Siemens 3 T Magnetom Trio MRI scanner (Siemens, Erlangen, Germany) with an 8 channel head coil was used for acquisition of single shot spin-echo diffusion weighted images (TR = 8700 msec, TE = 116 msec, 58 sagittal 2.5 mm slices, in plane resolution 2.5 x 2.5 mm). Implemented b values were

700, 1000, and 2800 s/mm2, applied in 25, 40, and 75 uniformly distributed directions. In addition, 10 images without diffusion weighting (b0) were obtained. For details on DTI preprocessing, we refer to the supplementary materials section.

Tract-based spatial statistics (TBSS)

For voxel-based analyses of white matter structure across the whole brain we used TBSS, which is resistant to systematic group differences and allows for more sensitive statistical testing and objective interpretation[31]. All subjects' fractional anisotropy (FA) data were registered to a common space (the FA158 MNI space template) using combined affine and non-linear registrations. A mean FA image was created, eroded to a skeleton and thresholded at FA > 0.2. Each subject's aligned FA data were then projected onto this skeleton and the nonlinear warps and FA skeleton projections applied to the mean diffusivity (MD) images. Voxelwise statistical analyses were performed using 10,000 randomized permutations.

We compared FA and MD between subgroups while correcting for age (included as covariate of no interest), focusing on the comparison between freezers and non-freezers. We used a cluster forming threshold of $t>3.4$, resembling a one-tailed statistical threshold of $p<.001$. The 95th percentile was used as cluster-size threshold (at $p<.05$) and fully corrected for multiple comparisons across space[32].

Probabilistic tractography

To obtain a more sensitive picture of freezing-related white matter quality, probabilistic tractography was applied to key subcortical-cortical connections, previously indicated to play a role in FOG[7]. [33]. We used an acquisition scheme with multiple b-values and applied a probabilistic diffusion model (BEDPOSTX) in subject diffusion space to calculate probability distributions of fibre direction at each voxel[34, 35]. To account for the non-monoexponential diffusion decay curve resulting from multiple b-

values[36], we employed the continuous gamma distribution model in FSL, shown to outperform a simpler noise-floor model especially at the interfaces between brain tissues[33].

Constrained probabilistic tractography (PROBTRACKX) was initiated[37] from seven subcortical seed masks (caudate, putamen, pallidum, subthalamic nucleus, thalamus, pedunculopontine nucleus and middle cerebellar peduncle) towards nine cortical target masks covering the majority of frontal, motor, and sensory cortex: anterior cingulate gyrus, orbitofrontal cortex, middle frontal gyrus, superior frontal gyrus, primary motor and premotor cortex, sensory cortex (S1&S2) and the supplementary motor areas (preSMA and SMAproper). A mask was used to prevent tracts crossing the midline, determined in MNI space (for details see supplementary material) and transformed to subject diffusion space using the inverse of the registrations generated during TBSS. Starting from each voxel in the seed region, 10,000 samples were generated with a curvature threshold of 0.2 and the samples reaching the target mask were retained.

To determine the probable spatial trajectory of each tract, the maps representing the distribution of trajectories from seed to target were thresholded at a low level to remove noise (0.02% of the maximum value in the connectivity map), transformed to MNI space (using the TBSS registrations), binarized and summed across participants. Voxels that were present in > 95 % of control participants' maps were retained. The resulting MNI space tracts were used to extract the mean FA from each subjects' skeleton image generated during the TBSS analysis.

Mean FA and MD of each subcortico-cortical tract were compared between groups using t-tests and p-values with a Sidak-adjusted Bonferroni correction taking into account the total number of tracts (n=98) and interdependence (i.e. mean FA/MD correlation across tracts)[38]. FA and MD values of tracts with significant group differences were correlated with the NFOG-Q, UPDRS III and other clinical scores in freezers using Pearson correlations corrected for age (Statistica 8, StatSoft, Tulsa, OK). We prioritized controlling for age effects and therefore used Pearson rather than Spearman

correlations[39]. All analyses were run with and without LED as a covariate. As results were very similar, we report on the LED-uncorrected results (for LED-corrected results see Supplementary materials).

Results

Whole brain group differences

Table 2 and Figure 1 illustrate the whole brain group differences in FA and MD and their association with clinical scores in freezers. The freezer group showed local decreases in FA in clusters in the left (lobule VI) and right (Crus I, lobule VIIIb) hemisphere of the cerebellum as well as in the left temporal part of the superior longitudinal fasciculus compared to non-freezers. Freezers also demonstrated increased MD values in the right anterior part of the capsula interna and corona radiata, the superior frontal cortex and a left-hemispheric cluster in cerebellum Crus II in contrast to non-freezers. This pattern of mainly freezer/non-freezer differences was partly driven by the enhanced white matter structure in non-freezers compared to controls (see supplementary materials).

FA and MD of significant clusters did not correlate to FOG severity in freezers but co-varied with freezers' disease severity. More precisely, stronger decreases in cerebellar FA were related to higher LED scores ($R=-0.68$, $p=0.03$). In freezers, there was an additional positive correlation between increased MD values of the right anterior capsula interna and motor severity as measured by UPDRS scores ($R=0.78$, $p<0.01$).

Table 2: Altered white matter integrity in freezers as revealed by whole brain TBSS analysis and relation to disease profile

Cluster info						Mean *(SD)*			
Label	X	Y	Z	size	Z-max	**Controls**	**Freezers**	**Non-Freezers**	**Association with disease profile**
FA Freezers < Non-Freezers									
R cerebellum Crus I	20	-65	-34	59	5.35	0.34 (0.04)	0.29 (0.02)	0.34 (0.02)	NS
L cerebellum VI	-21	-63	-35	19	4.26	0.34 (0.03)	0.31 (0.03)	0.36 (0.03)	NS
R cerebellum VIIIb	11	-68	-32	16	4.54	0.30 (0.02)	0.27 (0.04)	0.33 (0.04)	R (FA, LED) = -0,68 (p=0,03)
L Temporal SLF	-48	-49	-3	15	4.62	0.41 (0.04)	0.38 (0.04)	0.45 (0.04)	NS
FA Freezers < Controls									
R MCP	16	-29	-32	37	6.05	0.67 (0.05)	0.56 (0.05)	0.61 (0.06)	NS
MD Freezers > Non-Freezers						Mean x E-04 *(SD) x E-04*			
R anterior capsula interna	22	17	8	31	4.66	4.91 (0.29)	5.29 (0.56)	4.78 (2.13)	R(MD, UPDRS III) = 0,78 (p=0,008)
R superior frontal cortex	12	47	36	23	5.42	5.56 (0.39)	5.75 (0.42)	5.16 (0.27)	NS
L anterior thalamic radiation	-18	19	-2	13	4.47	5.41 (0.23)	5.81 (0.54)	5.26 (0.27)	NS
R anterior corona radiate	27	16	10	11	3.86	4.84 (0.39)	5.16 (0.47)	4.67 (0.27)	NS
L cerebellum Crus II	-11	-70	-35	11	4.66	4.37 (0.21)	4.62 (0.38)	4.30 (0.16)	NS

Table 2: Altered white matter integrity in freezers as revealed by whole brain TBSS analysis and relation to disease profile

The presented group comparisons are significant based on one-tailed t-tests in FSL with age as covariate and $p<0.05$ with FDR correction for multiple comparisons. Pearson brain-behavior correlations are corrected for age. Lower FA and higher MD values indicate poorer white matter integrity. Mean MD and SD values ranged between 0.00039 - 0.00066 and 0,0000162 – 0.0000541 respectively and are displayed as numbers x E-04 for clarity. FA= Fractional Anisotropy; MD= Mean diffusivity; SLF; Superior Longitudinal Fasciculus; MCP: Middle Cerebellar Peduncule; LED: Levodopa Equivalent Dose; NS: Not Significant.

Insert Figure 1 about here

Whole brain group differences

Tractography

Using a more focused analysis through probabilistic tractography, significant group differences in FA of subcortico-cortical tracts were found in connections between the left caudate nucleus and

anterior cingulate and orbitofrontal cortex as well as between the left middle cerebellar peduncle and pedunculopontine nucleus, with lower FA in freezers (See table 3 and figure 2A for details). More pronounced decreases in caudate-anterior cingulate cortex FA were correlated with more severe motor symptoms in freezers indicating a negative correlation (R= -0.66, p=0.038).

Similar to the results obtained through whole brain analysis, MD metrics were more sensitive to freezing-related changes in white matter, showing a consistent increase in MD in tracts connecting the caudate, putamen, pallidum and subthalamic nucleus to frontal (anterior cingulate cortex, superior and orbitofrontal cortex), motor (pre-supplementary motor area, supplementary motor area) and sensory (S1&S2) cortical regions predominantly in the left hemisphere (see Table 3 and figure 2B for details). Higher MD scores in freezers were predictive of higher UPDRS III scores, especially in cortical connections with the caudate nucleus (Figure 2C). No further associations with FOG severity or other clinical variables were found.

Table 3: Increased mean diffusivity of subcortico-cortical tracts in Freezers and relation to disease profile

Tracts			Mean x E-04 (SD x E-04)				
Subcortical ROI	**Cortical ROI**	**Hemisphere**	**Controls**	**Freezers**	**Non-Freezers**	**P-value**	**UPDRS III**
Caudate	ACC	Left	5.00 (0.30)	5.09 (0.37)	4.9 (0.23)	**0.001**	**0.65***
	OFC	Left	5.23 (0.29)	5.29 (0.30)	5.15 (0.20)	**<0.001**	0.58
		Right	5.10 (0.27)	5.20 (0.30)	5.00 (0.26)	**0.008**	0.58
	SFG	Left	4.87 (0.30)	4.93 (0.36)	4.77 (0.22)	**0.004**	**0.63***
	S12	Left	4.86 (0.39)	4.81 (0.26)	4.71 (0.24)	**0.006**	0.38
	preSMA	Left	4.90 (0.33)	4.93 (0.35)	4.78 (0.22)	**0.009**	**0.69***
	SMA	Left	4.83 (0.39)	4.82 (0.33)	4.69 (0.25)	**0.008**	0.55
Putamen	ACC	Left	4.80 (0.30)	4.86 (0.35)	4.71 (0.21)	**0.004**	0.57
		Right	5.55 (0.31)	5.56 (0.33)	5.34 (0.21)	**0.009**[1]	0.35
	OFC	Left	5.02 (0.29)	5.06 (0.31)	4.93 (0.17)	**0.007**	0.57
	MFG	Left	4.89 (0.33)	5.01 (0.45)	4.80 (0.22)	**0.005**	0.61
	SFG	Left	4.78 (0.29)	4.83 (0.35)	4.68 (0.20)	**0.005**	0.59
	M1	Left	4.86 (0.36)	4.87 (0.33)	4.74 (0.21)	**0.004**	0.49
		Right	4.89 (0.30)	4.91 (0.90)	4.78 (0.22)	**0.013**	0.60
	S12	Left	4.92 (0.34)	4.99 (0.37)	4.83 (0.21)	**0.003**	0.50
	PMC	Left	4.77 (0.38)	4.78 (0.35)	4.66 (0.24)	**0.007**	0.50
	preSMA	Left	4.76 (0.30)	4.82 (0.36)	4.65 (0.21)	**0.007**	0.61
	SMA	Left	4.72 (0.34)	4.73 (0.33)	4.61 (0.21)	**0.006**	0.53
Pallidum	ACC	Left	4.42 (0.29)	4.43 (0.33)	4.31 (0.19)	**0.015**	**0.63***
	OFC	Left	4.67 (0.30)	4.75 (0.33)	4.57 (0.21)	**0.001**	0.59
	SFG	Left	4.78 (0.26)	4.50 (0.31)	4.38 (0.19)	**0.014**	0.60
STN	OFC	Left	4.65 (0.33)	4.72 (0.37)	4.55 (0.27)	**0.003**	0.58

Table 3: Increased mean diffusivity of subcortico-cortical tracts in Freezers and relation to disease profile.

Bold p-values indicate significant MD increases in Freezers compared to Non-Freezers based on two-tailed t-tests corrected for age and multiple comparisons (Bonferonni-adjusted $p<0.01574$). Other group comparisons (Non-Freezers versus Controls; Freezers versus Controls) were not significant except for the right Putamen-ACC tract[1] where Freezers had increased MD compared to Non-Freezers as well as Controls. Higher MD values indicate poorer white matter integrity. * indicates significant associations ($p<0.05$) between increased MD and increased UPDRS motor scores in Freezers based on Pearson correlations in the Freezer group corrected for age. Mean MD and SD values ranged between 0.000326 - 0.00066 and 0,00000926 – 0.000648 respectively and are displayed as numbers *E-04 for clarity. MD= Mean diffusivity; ACC: Anterior Cingulate Cortex; OFC: Orbitofrontal Cortex; MFG: Middle Frontal Gyrus; SFG: Superior Frontal Gyrus; M1: Primary Motor Cortex; S12: Primary and Secondary Somatosensory Cortex; PMC: Premotor Cortex; SMA: Supplementary Motor Area; STN: Subthalamic Nucleus.

Insert Figure 2 about here

Tractography

Discussion

In this study, we used two complementary DTI methods to investigate FA and MD as indirect markers of white matter microstructure in PD patients with and without FOG and healthy controls. Group differences revealed that FOG is associated with distributed decreases in FA and increases in MD, believed to be indicative of structural white matter decline[40]. Besides corroborating FOG-related changes in brainstem and cerebellar white matter[25, 26], the results provide new evidence for white matter pathology in freezers affecting the intrahemispheric cortico-cortical association fibres of the superior longitudinal fasciculus, the motor-related corticofugal tract (capsula interna, anterior corona radiata) and substantial tracts connecting the striatum, subthalamic nucleus and thalamus (thalamic radiation) to motor, sensory and cognitive frontal regions. White matter alterations in freezers correlated to a more advanced disease profile, rather than increased FOG severity.

Microstructural changes in white matter are commonly reported in PD and may be more pronounced than grey matter alterations or even antedate them[41]. The exact underlying mechanism is unclear, although alpha-synucleinopathy leading to the characteristic dopaminergic denervation is thought to negatively impact on structural boundaries of white matter fibres[42]. As a result, the directionality and total magnitude of diffusion of water molecules along white matter tracts is changed. With MD being more sensitive to group differences than FA metrics, microstructural alterations in PD reportedly spread through subcortical white matter including the substantia nigra, striatum, capsula interna, thalamus, superior cerebellar peduncle[43-46] and fronto-parieto-temporal (superior longitudinal

fasciculus) and interhemispheric (corpus callosum) connections[45, 47-49]. While the majority of these tracts likely contribute to locomotor control[45], only two DTI studies reported an association with gait in PD irrespective of FOG. Marumoto et al.[50] found that gait speed was predicted by diffusion properties of the anterior thalamic radiation. Interestingly, this tract projects from the thalamus to frontal motor areas including the supplementary motor area and showed increased MD in freezers in the current study. Similarly, Lenfeldt et al.[51] showed that thalamic diffusion differentiated tremor-dominant from postural-instability and gait disorder phenotypes. However, the burden of white matter hyperintensities proved not different between these phenotypes in a large cohort study.[52]

White matter changes in PD have been consistently linked to Hoehn and Yahr disease staging[42, 51], self-efficacy, mental status[51] and depression[53]. As a much investigated biomarker of cognitive decline, white matter abnormalities were also related to the development of executive dysfunction, mild cognitive impairment and dementia[41, 42, 54]

A novel finding of the current study was that patients with FOG had reduced FA in the temporal part of the cortico-cortical association (superior longitudinal fasciculus) tract. The superior longitudinal fasciculus consists of bidirectional fibres that connect frontal with parietal and temporal areas. In PD, damage to this fasciculus has been linked to impaired motor preparation and visuospatial processing[44, 55, 56], deficits which are also prominent in patients with FOG[12, 13]. According to the recent anatomical subdivision of the human superior longitudinal fasciculus[57], the temporal cluster likely constitutes part of the arcuate fascicle which facilitates the modulation of attention towards sensory and spatial input through prefrontal connections.

The present study further revealed a distributed pattern of white matter damage in patients with FOG, including cerebellar regions, cerebello-pontine connections and subcortico-cortical connections. White matter abnormalities were more pronounced in freezers with a more severe disease profile, but no correlations with FOG severity were found. The narrow range of total NFOG-Q

scores (IQR 12.5-19.5) in the relatively small number of freezers (N=11) may have contributed to this finding.

Fling et al.[26] found no group differences in FA between freezers, non-freezers and controls using fibre tractography of the pedunculopontine nucleus. However, the volume of right-hemispheric white matter projections from the pedunculopontine nucleus to cerebellum, thalamus, basal ganglia and frontal motor-cognitive areas was reduced in freezers, but also proved not correlated to FOG-severity. Evaluating a broader scope of cerebral white matter, the present study confirms alterations in cerebellar regions and cerebello-pontine connections. Together with other recent findings [12, 14, 17], our results substantiate the importance of cerebellar and pedunculopontine nucleus involvement in FOG. Through widespread ascending and descending connections, the pedunculopontine nucleus may exert functional influences on both automatic as well as voluntary features of locomotion[3]. In contrast to Fling et al.[26], we do not confirm a predominantly right hemispheric white matter burden. If anything, our results point to left lateralisation, befitting the correlation of white matter changes with UPDRS motor scores. Fling et al. elucidated that the degree of inter-hemispheric asymmetry of the pedunculopontine nucleus network correlated to freezers' cognitive ability to selectively initiate and inhibit responses. These differences may be explained by the clinical test battery and DTI-analysis methods used, which in our study included a whole-brain comparison and subcortico-cortical probabilistic tractography.

As for the cerebellum, a recent review highlighted its compensatory role to maintain motor performance in PD[58]. Freezers may be less able to functionally recruit cerebellar networks due to altered white matter structure and as a result show gait impairment. FA in the cerebellum also related to LED in freezers. Although the direct influence of dopaminergic medication on structural brain connectivity is currently unknown, it is possible that the different medication profiles of the subgroups influenced white matter structures differently with time.

Though group differences in white matter cannot capture the episodic nature of a freezing event, the topographic pattern of white matter damage in typical motor and cognitive regions supports striatofrontal involvement in FOG[59]. Hence, white matter changes may reflect the background disease profile of patients who develop FOG. A surprising finding of this study was that non-freezers tended to show better white matter structure than controls, possibly signifying a specific pattern of functional reorganization in this patient group. Indeed, altered functional connectivity in the sensorimotor, cognitive and limbic networks has been shown to differ with disease severity[60, 61]. An alternative explanation points to the limitation of the diffusion tensor model, estimating the principal diffusion direction in each voxel and not accounting for crossing fibers. In addition, white matter hyperintensity burden may have influenced the findings, despite recent studies suggesting no relationship with freezing of gait[52]. Future study needs to include both DTI and Fluid Attenuated Inversion Recovery (FLAIR) sequences to control for this possible confounder, using the most recent acquisition and analysis protocols to overcome the crossing fiber problems[62]. Most importantly, analysis of white matter changes over time in conjunction with functional connectivity is imperative to fully understand the emergence of FOG.

Conclusion

We provide novel data showing that the topographic pattern of FOG-related microstructural atrophy extends to intrahemispheric cortico-cortical, motor-related corticofugal and several basal ganglia white matter tracts projecting to motor, sensory and cognitive frontal areas.

Abbreviations

DTI: diffusion tensor imaging; **FA**: fractional anisotropy; **fMRI**: functional Magnetic Resonance Imaging; **FOG**: Freezing of gait; **FSL**: FMRIB Software Library; **LED**: Levodopa equivalent dose; **MD**: mean diffusivity; **MMSE**: Mini Mental State Examination; **NFOG-Q**: new Freezing of Gait-Questionnaire; **S1**: primary sensory cortex; **S2**: secondary sensory cortex; **SCOPA-COG**: cognitive section of the Scales for Outcomes in PD; **TBSS**: tract-based spatial statistics; **TE**: echo time; **TR**: repetition time; **UPDRS**: Unified Parkinson's Disease Rating Scale.

Acknowledgments

We are grateful to all subjects and Parkinson patients in particular for their willingness to participate. Many thanks go to N. Rentmeesters for his assistance during testing. Support for this study was provided through a grant from the Special Research Fund of KU Leuven, Belgium (contract OT / 11/ 09 and the Malou-Malou funds King Baudouin foundation. I. L. is supported by a research grant of the Research Foundation – Flanders (F.W.O). Conflict of Interest: All authors report no conflict of interest. W.V. is a Senior Clinical Investigator of the F.W.O.

Author roles

1.Research project: A. Conception, B. Organization, C. Execution;

2.Statistical Analysis: A. Design, B. Execution, C. Review and Critique;

3.Manuscript Preparation: A. Writing of the first draft, B. Review and Critique;

Vercruysse S: 1A; 1B; 1C; 2A; 2B; 3A

Leunissen I: 2A; 2B; 3B

Vervoort G: 2C; 3B,

Vandenberghe W: 1B; 2C; 3B

Swinnen S: 1A; 2C; 3B

Nieuwboer A: 1A; 1B; 2A; 2C; 3B

References

1. Kerr GK, Worringham CJ, Cole MH, Lacherez PF, Wood JM, Silburn Pa. Predictors of future falls in Parkinson disease. Neurology 2010;75(2):116-124.
2. Perez-Lloret S, Negre-Pages L, Damier P, et al. Prevalence, determinants, and effect on quality of life of freezing of gait in Parkinson disease. JAMA Neurol 2014;71(7):884-890.
3. Nutt JG, Bloem BR, Giladi N, Hallett M, Horak FB, Nieuwboer A. Freezing of gait: moving forward on a mysterious clinical phenomenon. Lancet Neurol 2011;10(8):734-744.
4. Giladi N, Treves Ta, Simon ES, et al. Freezing of gait in patients with advanced Parkinson's disease. Journal of Neural Transmission 2001;108(1):53-61.
5. Matsui H, Udaka F, Miyoshi T, et al. Three-dimensional stereotactic surface projection study of freezing of gait and brain perfusion image in Parkinson's disease. Mov Disord 2005;20(10):1272-1277.
6. Herman T, Giladi N, Hausdorff JM. Neuroimaging as a window into gait disturbances and freezing of gait in patients with Parkinson's disease. Curr Neurol Neurosci Rep 2013;13(12):411.
7. Herman T, Giladi N, Hausdorff JM. Neuroimaging as a window into gait disturbances and freezing of gait in patients with Parkinson's disease. Current neurology and neuroscience reports 2013;13(12):411-411.
8. Imamura K, Okayasu N, Nagatsu T. Cerebral blood flow and freezing of gait in Parkinson's disease. Acta Neurol Scand 2012;126(3):210-218.
9. Bartels AL, de Jong BM, Giladi N, et al. Striatal dopa and glucose metabolism in PD patients with freezing of gait. Mov Disord 2006;21(9):1326-1332.
10. Tessitore A, Amboni M, Esposito F, et al. Resting-state brain connectivity in patients with Parkinson's disease and freezing of gait. Parkinsonism Relat Disord 2012;18(6):781-787.
11. Fling BW, Cohen RG, Mancini M, et al. Functional reorganization of the locomotor network in Parkinson patients with freezing of gait. PLoS One 2014;9(6):e100291.
12. Snijders AH, Leunissen I, Bakker M, et al. Gait-related cerebral alterations in patients with Parkinson's disease with freezing of gait. Brain : a journal of neurology 2011;134(Pt 1):59-72.
13. Peterson DS, Pickett KA, Duncan R, Perlmutter J, Earhart GM. Gait-related brain activity in people with Parkinson disease with freezing of gait. PLoS One 2014;9(3):e90634.
14. Shine JM, Matar E, Ward PB, et al. Differential neural activation patterns in patients with Parkinson's disease and freezing of gait in response to concurrent cognitive and motor load. PLoS One 2013;8(1):e52602.
15. Vercruysse S, Spildooren J, Heremans E, et al. The Neural Correlates of Upper Limb Motor Blocks in Parkinson's Disease and Their Relation to Freezing of Gait. Cerebral cortex (New York, NY : 1991) 2013.
16. Handojoseno AM, Shine JM, Nguyen TN, Tran Y, Lewis SJ, Nguyen HT. Using EEG spatial correlation, cross frequency energy, and wavelet coefficients for the prediction of Freezing of Gait in Parkinson's Disease patients. Conf Proc IEEE Eng Med Biol Soc 2013;2013:4263-4266.
17. Shine JM, Matar E, Ward PB, et al. Exploring the cortical and subcortical functional magnetic resonance imaging changes associated with freezing in Parkinson's disease. Brain 2013;136(Pt 4):1204-1215.
18. Shine JM, Matar E, Ward PB, et al. Freezing of gait in Parkinson's disease is associated with functional decoupling between the cognitive control network and the basal ganglia. Brain 2013;136(Pt 12):3671-3681.
19. Maidan I, Bernad-Elazari H, Brozgol M, Giladi N, Mirelman A, Hausdorff J. Increased activation of the frontal lobe is associated with freezing of gait in patients with Parkinson's disease: an fNIRS study. Proceedings of the International Society for Posture & Gait Research; 2013.
20. Shine JM, Handojoseno AM, Nguyen TN, et al. Abnormal patterns of theta frequency oscillations during the temporal evolution of freezing of gait in Parkinson's disease. Clin Neurophysiol 2014;125(3):569-576.

21. Vercruysse S, Gilat M, Shine JM, Heremans E, Lewis S, Nieuwboer a. Freezing beyond gait in Parkinson's disease: a review of current neurobehavioral evidence. Neuroscience and biobehavioral reviews 2014;43:213-227.
22. Kostic VS, Agosta F, Pievani M, et al. Pattern of brain tissue loss associated with freezing of gait in Parkinson disease. Neurology 2012;78(6):409-416.
23. Tessitore A, Amboni M, Cirillo G, et al. Regional gray matter atrophy in patients with Parkinson disease and freezing of gait. AJNR Am J Neuroradiol 2012;33(9):1804-1809.
24. Herman T, Rosenberg-Katz K, Jacob Y, Giladi N, Hausdorff JM. Gray matter atrophy and freezing of gait in Parkinson's disease: Is the evidence black-on-white? Mov Disord 2014;29(1):134-139.
25. Schweder PM, Hansen PC, Green AL, Quaghebeur G, Stein J, Aziz TZ. Connectivity of the pedunculopontine nucleus in parkinsonian freezing of gait. Neuroreport 2010;21(14):914-916.
26. Fling BW, Cohen RG, Mancini M, Nutt JG, Fair DA, Horak FB. Asymmetric pedunculopontine network connectivity in parkinsonian patients with freezing of gait. Brain 2013;136(Pt 8):2405-2418.
27. Nieuwboer A, Rochester L, Herman T, et al. Reliability of the new freezing of gait questionnaire: agreement between patients with Parkinson's disease and their carers. Gait Posture 2009;30(4):459-463.
28. Fahn S, Elton R, Committee UD. Unified Parkinson's Disease Rating Scale. In: Fahn S, Marsden CD, Calne DB, Goldstein M. Eds. Recent developments in Parkinson's Disease; 1987. p. p153-163.
29. Hoehn MM, Yahr MD. Parkinsonism: onset, progression and mortality. Neurology 1967;17(5):427-442.
30. Marinus J, Visser M, Verwey NA, et al. Assessment of cognition in Parkinson's disease. Neurology 2003;61(9):1222-1228.
31. Smith SM, Jenkinson M, Johansen-Berg H, et al. Tract-based spatial statistics: voxelwise analysis of multi-subject diffusion data. Neuroimage 2006;31(4):1487-1505.
32. Jbabdi S, Behrens TE, Smith SM. Crossing fibres in tract-based spatial statistics. Neuroimage 2010;49(1):249-256.
33. Jbabdi S, Sotiropoulos SN, Savio AM, Graña M, Behrens TE. Model-based analysis of multishell diffusion MR data for tractography: how to get over fitting problems. Magn Reson Med 2012;68(6):1846-1855.
34. Behrens TE, Berg HJ, Jbabdi S, Rushworth MF, Woolrich MW. Probabilistic diffusion tractography with multiple fibre orientations: What can we gain? Neuroimage 2007;34(1):144-155.
35. Behrens TE, Woolrich MW, Jenkinson M, et al. Characterization and propagation of uncertainty in diffusion-weighted MR imaging. Magn Reson Med 2003;50(5):1077-1088.
36. Niendorf T, Dijkhuizen RM, Norris DG, van Lookeren Campagne M, Nicolay K. Biexponential diffusion attenuation in various states of brain tissue: implications for diffusion-weighted imaging. Magn Reson Med 1996;36(6):847-857.
37. Leunissen I, Coxon JP, Caeyenberghs K, Michiels K, Sunaert S, Swinnen SP. Task switching in traumatic brain injury relates to cortico-subcortical integrity. Hum Brain Mapp 2014;35(5):2459-2469.
38. Abdi H. Bonferroni and Šidák corrections for multiple comparisons.(http://www.utdallas.edu/~herve/Abdi-Bonferroni2007-pretty.pdf) In N.J. Salkind (ed.). Encyclopedia of Measurement and Statistics.Thousand Oaks, CA: Sage.
39. Lebel C, Gee M, Camicioli R, Wieler M, Martin W, Beaulieu C. Diffusion tensor imaging of white matter tract evolution over the lifespan. Neuroimage 2012;60(1):340-352.
40. Basser PJ. Inferring microstructural features and the physiological state of tissues from diffusion-weighted images. NMR Biomed 1995;8(7-8):333-344.
41. Duncan GW, Firbank MJ, O'Brien JT, Burn DJ. Magnetic resonance imaging: a biomarker for cognitive impairment in Parkinson's disease? Mov Disord 2013;28(4):425-438.
42. Agosta F, Canu E, Stefanova E, et al. Mild cognitive impairment in Parkinson's disease is associated with a distributed pattern of brain white matter damage. Hum Brain Mapp 2014;35(5):1921-1929.
43. Chan LL, Rumpel H, Yap K, et al. Case control study of diffusion tensor imaging in Parkinson's disease. J Neurol Neurosurg Psychiatry 2007;78(12):1383-1386.
44. Gattellaro G, Minati L, Grisoli M, et al. White matter involvement in idiopathic Parkinson disease: a diffusion tensor imaging study. AJNR Am J Neuroradiol 2009;30(6):1222-1226.

45. Kim HJ, Kim SJ, Kim HS, et al. Alterations of mean diffusivity in brain white matter and deep gray matter in Parkinson's disease. Neurosci Lett 2013;550:64-68.
46. Péran P, Cherubini A, Assogna F, et al. Magnetic resonance imaging markers of Parkinson's disease nigrostriatal signature. Brain 2010;133(11):3423-3433.
47. Agosta F, Pievani M, Svetel M, et al. Diffusion tensor MRI contributes to differentiate Richardson's syndrome from PSP-parkinsonism. Neurobiol Aging 2012;33(12):2817-2826.
48. Karagulle Kendi AT, Lehericy S, Luciana M, Ugurbil K, Tuite P. Altered diffusion in the frontal lobe in Parkinson disease. AJNR Am J Neuroradiol 2008;29(3):501-505.
49. Rae CL, Correia MM, Altena E, Hughes LE, Barker RA, Rowe JB. White matter pathology in Parkinson's disease: the effect of imaging protocol differences and relevance to executive function. Neuroimage 2012;62(3):1675-1684.
50. Marumoto K, Koyama T, Hosomi M, Kodama N, Miyake H, Domen K. Diffusion tensor imaging in elderly patients with idiopathic normal pressure hydrocephalus or Parkinson's disease: diagnosis of gait abnormalities. Fluids Barriers CNS 2012;9(1):20.
51. Lenfeldt N, Hansson W, Larsson A, Nyberg L, Birgander R, Forsgren L. Diffusion tensor imaging and correlations to Parkinson rating scales. J Neurol 2013;260(11):2823-2830.
52. Herman T, Rosenberg-Katz K, Jacob Y, et al. White matter hyperintensities in Parkinson's disease: do they explain the disparity between the postural instability gait difficulty and tremor dominant subtypes? PLoS One 2013;8(1):e55193.
53. Kostić VS, Agosta F, Petrović I, et al. Regional patterns of brain tissue loss associated with depression in Parkinson disease. Neurology 2010;75(10):857-863.
54. Koshimori Y, Segura B, Christopher L, et al. Imaging changes associated with cognitive abnormalities in Parkinson's disease. Brain Struct Funct 2014.
55. Farina E, Gattellaro G, Pomati S, et al. Researching a differential impairment of frontal functions and explicit memory in early Parkinson's disease. Eur J Neurol 2000;7(3):259-267.
56. Brück A, Kurki T, Kaasinen V, Vahlberg T, Rinne JO. Hippocampal and prefrontal atrophy in patients with early non-demented Parkinson's disease is related to cognitive impairment. J Neurol Neurosurg Psychiatry 2004;75(10):1467-1469.
57. Makris N, Kennedy DN, McInerney S, et al. Segmentation of subcomponents within the superior longitudinal fascicle in humans: a quantitative, in vivo, DT-MRI study. Cereb Cortex 2005;15(6):854-869.
58. Wu T, Hallett M. The cerebellum in Parkinson's disease. Brain 2013;136(Pt 3):696-709.
59. Shine JM, Moustafa AA, Matar E, Frank MJ, Lewis SJ. The role of frontostriatal impairment in freezing of gait in Parkinson's disease. Front Syst Neurosci 2013;7:61.
60. Tessitore A, Giordano A, De Micco R, Russo A, Tedeschi G. Sensorimotor connectivity in Parkinson's disease: the role of functional neuroimaging. Front Neurol 2014;5:180.
61. Kurani AS, Seidler RD, Burciu RG, et al. Subthalamic nucleus-sensorimotor cortex functional connectivity in de novo and moderate Parkinson's disease. Neurobiology of aging 2014:1-8.
62. Tournier JD, Yeh CH, Calamante F, Cho KH, Connelly A, Lin CP. Resolving crossing fibres using constrained spherical deconvolution: validation using diffusion-weighted imaging phantom data. Neuroimage 2008;42(2):617-625.

1 **Figures**

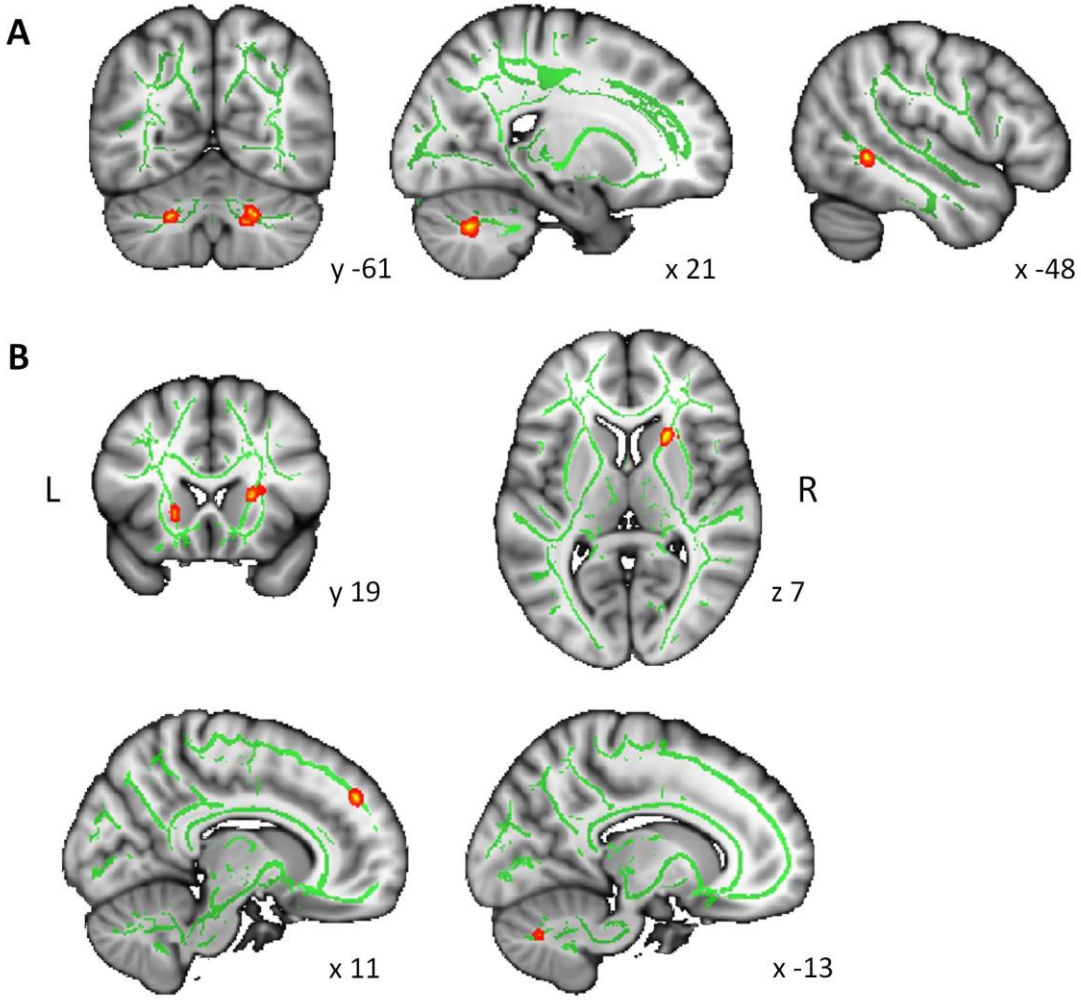
A
y -61
x 21
x -48
B
L
y 19
z 7
R
x 11
x -13

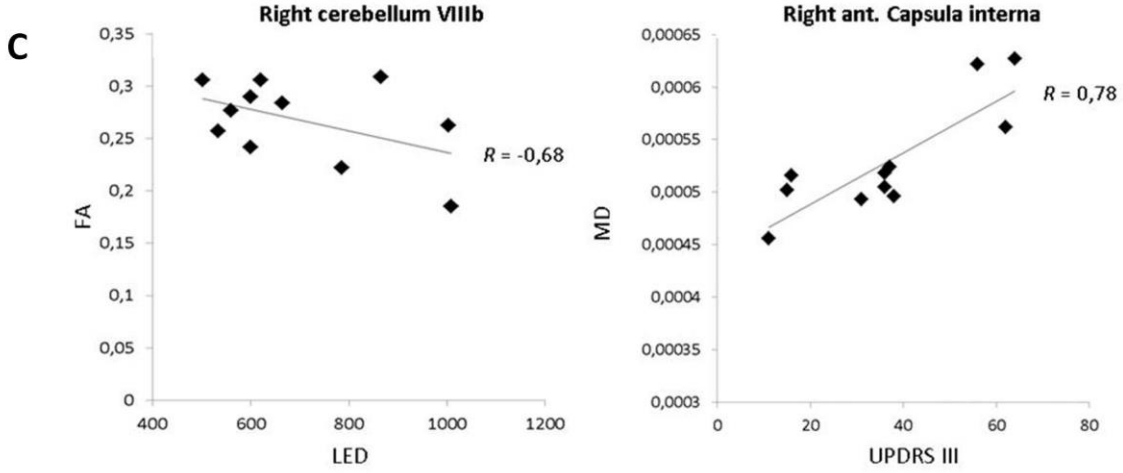
C
Right cerebellum VIIIb
FA
LED
R = -0,68
Right ant. Capsula interna
MD
UPDRS III
R = 0,78

Figure 1 Group differences in white matter structure across the whole brain and their association to disease profiles in freezers. Clusters with significantly reduced FA (**A**) and increased MD (**B**) in the freezer group compared to Non-Freezers overlaid on the TBSS skeleton (green). (Cluster threshold t>3.4, P<0.05 corrected for multiple comparisons). See Table 2 for cluster coordinates and group mean values. Part **C** shows the association between FA in the right cerebellar part VIIIb and levodopa equivalent dose (LED) values in the freezer group (left scatter plot) and the association between MD of the anterior part of the right capsula interna and UPDRS III motor scores in the freezer group (right scatter plot). Pearson correlations are significant at p<0,05 and corrected for age.

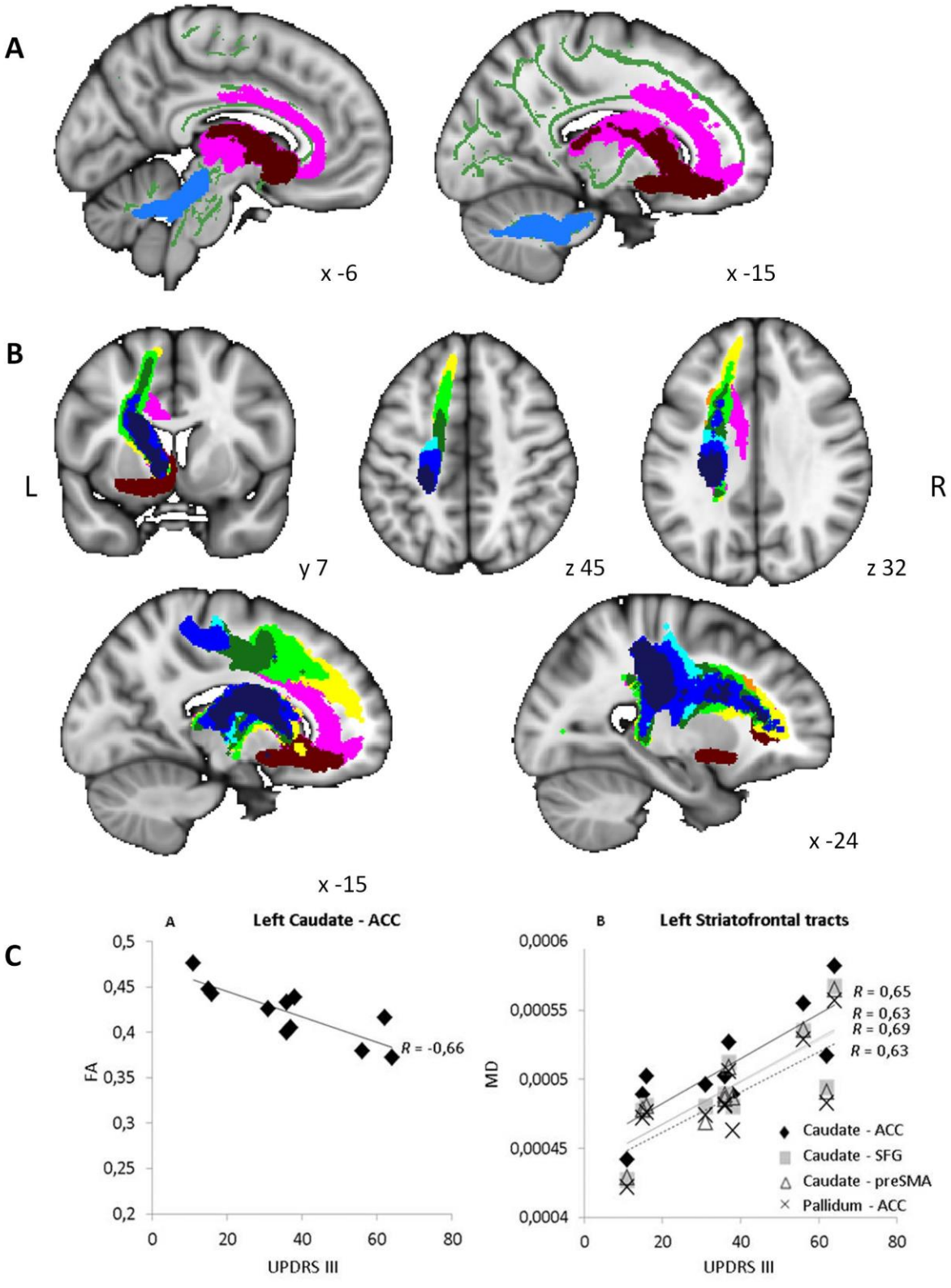
A
x -6
x -15
B
L
R
y 7
z 45
z 32
x -24
x -15
C
A
Left Caudate - ACC
FA
UPDRS III
R = -0,66
B
Left Striatofrontal tracts
MD
UPDRS III
R = 0,65
R = 0,63
R = 0,69
R = 0,63
Caudate - ACC
Caudate - SFG
Caudate - preSMA
Pallidum - ACC

1

Figure 2 Group differences in white matter structure of striatofrontal tracts and their association with disease profiles in freezers. Striatofrontal tracts with significantly reduced FA **(A)** and increased MD **(B)** in the freezer group. For clarity, the TBSS skeleton (green in part A) is removed in part B. See Table 3 for corresponding Bonferroni-corrected p-values and anatomical details. Part **C** depicts the association between FA in the left caudate –ACC tract and UPDRS III motor scores in the freezer group (left scatter plot). The right scatter plot depicts the association between MD of left striatofrontal tracts and UPDRS III motor scores in the freezer group. Pearson correlations are significant at p<0,05 and corrected for age. ACC: Anterior Cingulate Cortex; SFG: Superior Frontal Gyrus; SMA: Supplementary Motor Area.